Journal of Materials Science and Chemical Engineering, 2026, 14(11), 1-19
https://www.scirp.org/journal/msce
ISSN Online: 2327-6053
ISSN Print: 2327-6045

Mechanical Characterization of Compressed Earth Block Reinforced with Rhecktophyllum Camerunense Fiber

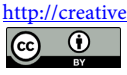
Jaques Bertrand Sombga[1], Jean Calvin Bidoung[1,2,3], Lucien Meva'a[1,2]

[1]Solid Mechanics Laboratory, National Advanced School of Engineering, Yaounde, Cameroon
[2]National Advanced School of Engineering, Yaounde, Cameroon
[3]Local Materials Promotion Authority, Yaounde, Cameroon
Email: jbsombga@gmail.com

How to cite this paper: Sombga, J.B., Bidoung, J.C. and Meva'a, L. (2026) Mechanical Characterization of Compressed Earth Block Reinforced with Rhecktophyllum Camerunense Fiber. *Journal of Materials Science and Chemical Engineering*, **14**, 1-19.
https://doi.org/10.4236/msce.2026.1411001

Received: October 1, 2026
Accepted: November 2, 2026
Published: November 5, 2026

Copyright © 2026 by author(s) and Scientific Research Publishing Inc.
This work is licensed under the Creative Commons Attribution International License (CC BY 4.0).
http://creativecommons.org/licenses/by/4.0/



Open Access

Abstract

The use of earth as a sustainable building material offers major ecological and economic advantages, particularly in rural areas of Cameroon. However, its low mechanical properties limit its extended structural use. This study addresses the physical and mechanical characterization of Compressed Earth Blocks (CEB) produced from three laterites from the Yaoundé region (Mbankomo, Nsimalen and Messamendongo), stabilized with cement (4%, 6%, and 8%) and reinforced with Rhecktophyllum camerunense (RC) plant fibers at contents of 0%, 0.5%, 1% and 1.5% by dry mass. The results show that the introduction of fibers generally reduces the bulk density by creating cavities, but increases compressive and flexural strength relative to the unreinforced control (CEB 0); Dunnett's test against the matched CEB 0 (same laterite, cement dosage and curing age) shows that this improvement is statistically significant ($p < 0.001$) in all 81 comparisons for both properties. The optimal formulation is obtained with Messamendongo laterite stabilized with 8% cement and reinforced with 1% RC fiber after 28 days of curing, reaching a maximum compressive strength of 14.87 ± 0.12 MPa (mean ± SD, n = 5), *i.e.* a gain of +144% over the matched unreinforced control (6.09 ± 0.18 MPa, n = 5; Dunnett $p < 0.001$). Two-way ANOVA including CEB 0 (fiber content 0% - 1.5% × cement dosage) shows significant effects of fiber content and cement dosage on compressive strength for every laterite and curing age tested ($p < 0.001$). Beyond 1% fiber content, a saturation and clogging effect generates clusters, reducing overall mechanical performance. The fibers also increase the initial water absorption rate owing to their hydrophilic nature.

Keywords

Compressed Earth Block, Rhecktophyllum Camerunense (RC) Fiber,

Compressive Strength, Flexural Strecngth

1. Introduction

Earth is one of humanity's oldest building materials. Earthen construction methods are varied and closely depend on geographic areas as well as historical periods. Over the centuries, the technology has evolved from "wattle and daub" to "maltoni," by way of "rammed earth" [1] [2]. The construction system known as "adobe," based on the use of sun-dried mud bricks to erect earthen buildings, has been documented in the Mediterranean region since ancient times [3] [4].

At present, it is estimated that about 30% of the world's population lives in earthen buildings [5]. The renewed interest in this material is based on the development of highly varied production techniques, supported by in-depth scientific research, illustrated in particular by Compressed Earth Block (CEB) technology [6]. Earth offers several undeniable advantages: ease of implementation, high local availability, excellent thermal conductivity (inertia), and low maintenance costs. Given these strengths, it is preferentially used for construction purposes, particularly in rural areas of developing countries. However, the raw use of earth presents specific constraints in terms of mechanical strength and weathering durability, which restricts its use on a wider scale. This is why this traditional material has been largely replaced by more solid industrial materials with a high carbon footprint.

Soil compaction significantly improves its initial mechanical properties. To offset water sensitivity and increase durability, the use of stabilizers (cement, lime, bitumen) or fibrous reinforcement has given rise to high-performance composite CEBs. The use of natural fibers currently enjoys real popularity in materials science. Several natural fibers have already been studied for reinforcing CEB properties, such as date palm, straw, banana and jute fibers [7]-[12]. In Cameroon, there is a wide variety of plant fibers, notably Rhecktophyllum camerunense (RC) fiber. This fiber was first identified by Colette Ntepe-Nyame in 1981 [13] and characterized in detail at the macro-structural level by Ntenga in 2007 [14]. It has also been successfully incorporated as a reinforcement in plaster matrices by Betene Ebanda in 2012 [15].

Over the past decade, the reinforcement of compressed earth blocks (CEB) with natural plant fibers has become an active research area, driven by the search for low-carbon, locally sourced alternatives to fired brick and concrete masonry [16] [17]. Several reviews have synthesized the mechanical behavior of CEB reinforced with fibers such as sisal, jute, coconut, kenaf, date palm, banana, bamboo and Alfa [16] [18]-[21], generally reporting three consistent trends: 1) fiber incorporation reduces bulk density owing to the low intrinsic density of plant fibers relative to mineral grains; 2) an optimal fiber content exists beyond which agglomeration, fiber bundling and increased porosity degrade mechanical performance; and 3) fiber bridging markedly improves flexural strength and post-cracking ductility

compared with unreinforced or purely cement-stabilized blocks.

Quantitatively, the reported optimal fiber contents and associated compressive strength gains vary widely with fiber type, soil mineralogy and cement dosage (Table 1). Bamboo (Bambusa vulgaris) fiber at 0.5 wt% and 4 cm length increased compressive strength by 43.6% relative to the unreinforced matrix [17]. Kenaf fiber studies report a similar optimum range of 0.5 wt% - 1.5 wt%, with porosity governed jointly by fiber length and concentration [17]. For sisal fiber - the most extensively studied natural fiber in cement-stabilized CEB - reported optimal contents cluster between 0.4% and 1.0% by mass combined with 8% - 10% cement, with peak compressive strengths ranging from about 4 MPa to over 13 MPa depending on soil type, fiber treatment and specimen geometry [22] [23]. Jute fiber, in contrast, has been reported to reduce compressive strength while improving crack resistance [16] [17], illustrating that the direction and magnitude of the fiber effect is fiber-specific rather than universal. Alfa fiber combined with crushed brick waste has also been shown to improve both the mechanical and thermal behavior of CEB [24].

Table 1. Indicative compressive strength gains reported for compressed earth blocks reinforced with different natural fibers.

Fiber	Reported optimal content	Reported effect on compressive strength	Reference
Bamboo (Bambusa vulgaris)	0.5 wt%, 4 cm length	+43.6% vs. unreinforced matrix	[17]
Kenaf	0.5 wt% - 1.5 wt%	Optimum governed by fiber length/porosity trade-off	[17]
Sisal	0.4 wt% - 1.0 wt% + 8 wt% - 10% cement	Peak $R_c \approx 4$ - 13+ MPa (soil- and treatment-dependent)	[22] [23]
Jute	0.5 wt% - 2 wt%	Can reduce R_c while improving crack resistance	[16] [17]
Sisal (+ crushed brick waste)	Soil-dependent	Improved mechanical and thermal behavior	[24]
Rhecktophyllum camerunense (this study)	1.0 wt% + 8% cement	R_c = 14.87 MPa (Messamendongo laterite, 28 d); +144.1% vs. matched CEB 0 (Dunnett, $p < 0.001$)	present study

The 14.87 MPa peak compressive strength obtained in the present study with 1% RC fiber and 8% cement compares favorably, in absolute terms, with the upper range reported for sisal-reinforced CEB, suggesting that RC fiber is a competitive candidate among tropical plant fibers for CEB reinforcement. This comparison should, however, be interpreted with caution given differences in soil mineralogy, specimen geometry and compaction method across studies, which several reviews identify as a persistent barrier to cross-study comparability in this field [17] [21]. Relative gains with respect to matched unreinforced controls are discussed in Section 3.4.

Despite this growing body of work, two gaps are apparent in the literature. First, African and Central African plant fibers remain comparatively under-studied relative to sisal, jute, coconut or kenaf, even though the continent hosts a wide diversity of cellulosic fibers with documented mechanical potential [13] [14]. Rhecktophyllum camerunense (RC) fiber, endemic to the Cameroonian rainforest, has been characterized at the fiber scale [14] and used successfully as a plaster reinforcement [15], but its behavior as a CEB reinforcement combined with ce-

ment stabilization had not previously been reported in the literature reviewed here. Second, a 2024 systematic review covering more than 120 CEB studies indicates that the reported research on CEB stabilizers and reinforcements generally lacks statistical treatment such as one-way ANOVA or Student's t-test to demonstrate the significance of the observed differences, and calls for future studies to report replicate-based descriptive statistics and significance testing [17]. The present study addresses both gaps by 1) characterizing RC fiber, a previously unreported reinforcement for CEB, across three lateritic soils and three cement dosages, and 2) situating the results within a statistically grounded design, discussed further in Section 2.5.

This study is organized into two main parts. First, we present the physical and geotechnical characteristics of the various materials used in the preparation of our CEB samples (laterites, cement, water and fibers). Second, we carry out an in-depth analysis of the impact of the formulation (RC fiber content and cement percentage) on the physical properties (porosity, absorption) and mechanical properties (three-point bending, compression) after 7, 14 and 28 days of curing [25]-[27], including the statistical significance of the observed differences (Section 2.5).

2. Materials and Methods

2.1. Materials Used

The main constituent of CEBs is lateritic soil. In this study, three laterites from three distinct geographic areas of Cameroon's Centre Region were used, namely:

- Mbankomo, in the Mefou-et-Akono department (**Figure 1**)

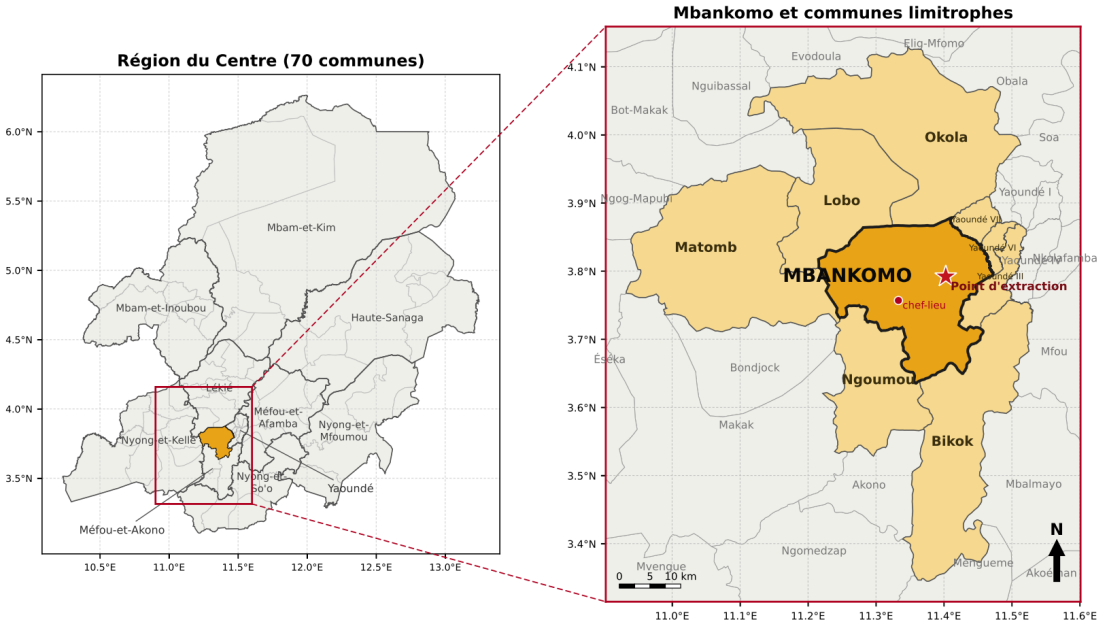


Figure 1. Geographic location of Mbankomo.

- Nsimalen, in the Mfou department (**Figure 2**)

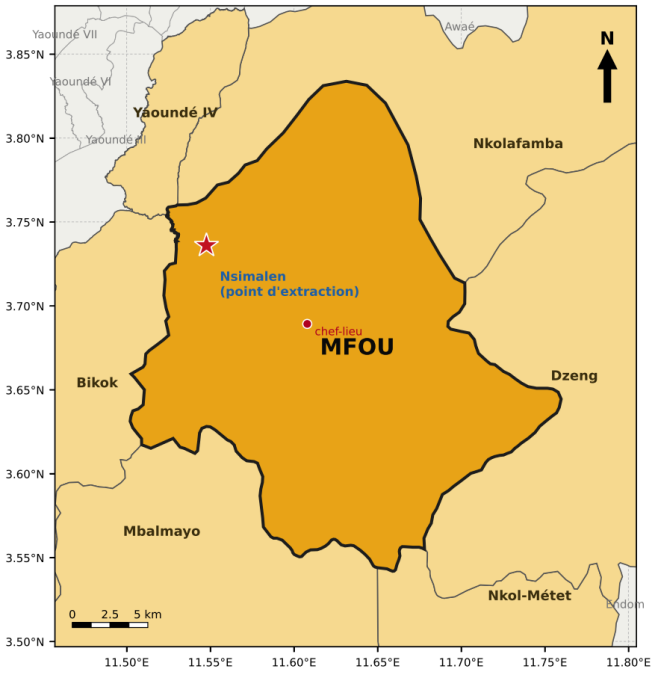


Figure 2. Geographic location of Mfou.

- Messamendongo, in the Mfoundi department, Yaoundé IV municipality (Figure 3)

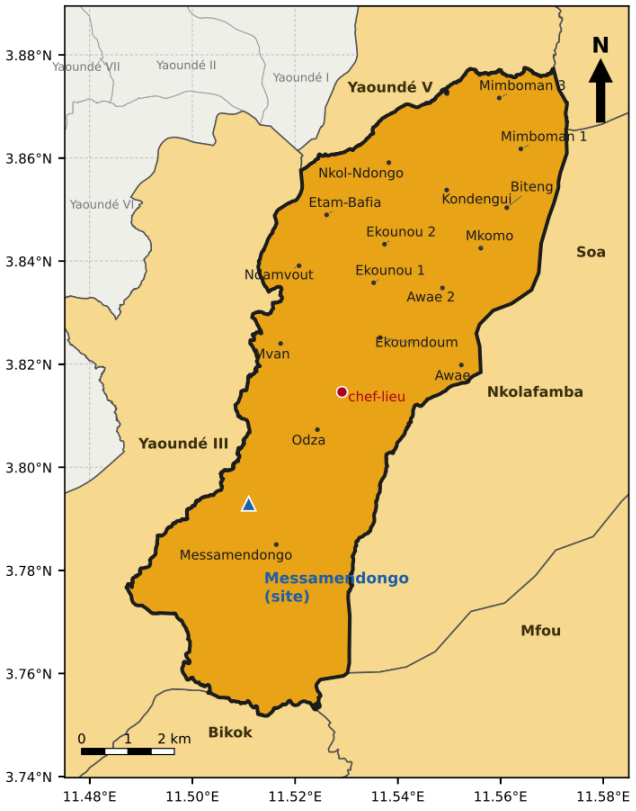
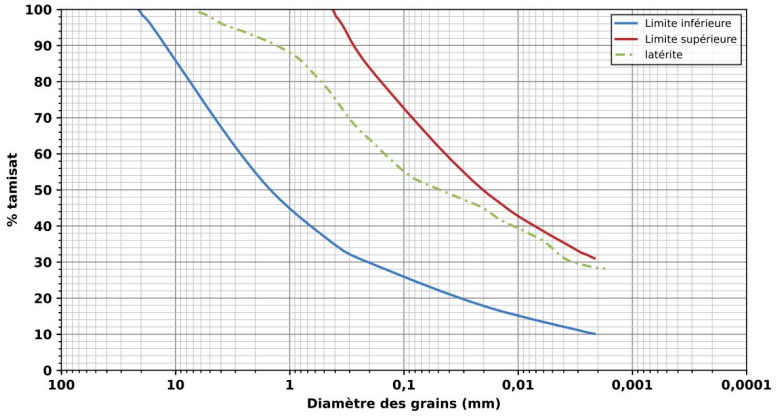
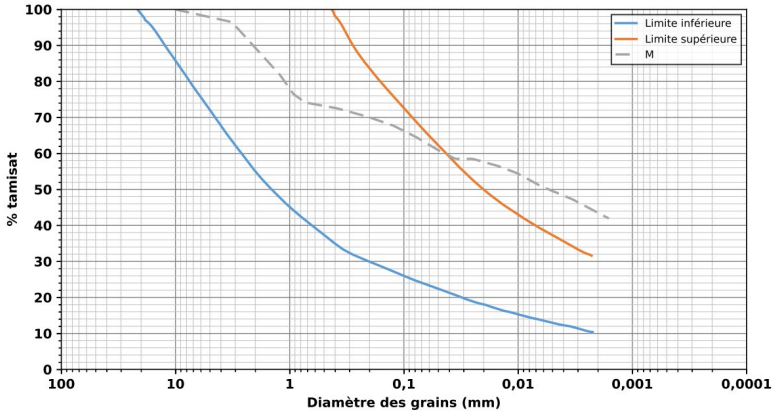


Figure 3. Geographic location of the Yaoundé IV municipality.

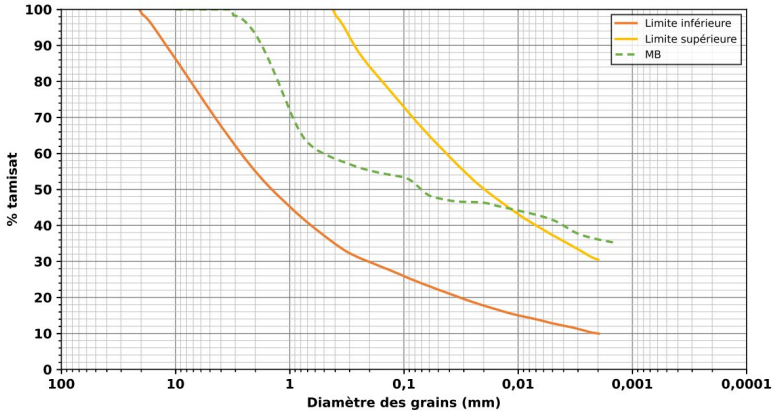
A complete particle-size analysis was carried out in accordance with standard NF P 94-056 to assess their compliance with the regulatory grading envelopes. The resulting particle-size distribution curves are shown in Figure 4.



(a)



(b)



(c)

Figure 4. Particle-size distribution curves of the laterites ((a)—Nsimalen laterite, (b)—Messamendongo laterite, (c)—Mbankomo laterite) relative to the grading envelopes of standard XP P 13-901 [28].

Analysis of the curves shows that only the Nsimalen laterite falls entirely within the particle-size limits recommended by the XP P 13-901 standard for compressed earth blocks. The Mbankomo and Messamendongo laterites present curves that partially fall outside these limits, requiring increased attention during stabilization.

The Atterberg limits define the intrinsic plasticity of a fine soil by measuring changes in consistency as a function of water content. The tests were carried out on the soil mortar (fraction below 0.4 mm) using the Casagrande apparatus, following the procedure of standard NF P 94-051 [29]. The geotechnical identification parameters are given in Table 2.

Table 2. Summary of the experimental Atterberg limits of the three Yaoundé laterites.

Parameter	Nsimalen	Messamendongo	Mbankomo
LL/Wl (%)	59.3 (Wl)	52.8 (Wl)	56.7 (Wl)
Wp (%)	36.8	31.8	36.2
Ip (%)	22.5	21.0	20.5

According to the Atterberg classification (recalled in Table 3), all three soil types fall into the "plastic" category ($15 < Ip < 40$), confirming their suitability for the cohesion required for CEB manufacturing.

Table 3. Regulatory plasticity thresholds according to the Atterberg classification [29].

Plasticity index (Ip)	Soil plasticity degree
$0 < Ip < 5$	Non-plastic (the test loses its significance)
$5 < Ip < 15$	Moderately plastic
$15 < Ip < 40$	Plastic
$Ip > 40$	Highly plastic

The particle-size compositions of our laterites are given in Table 4.

Table 4. Particle-size composition of the laterites (MIPROMALO).

Laterite	Color/appearance	Gravel $\Phi >$ 2 mm (%)	Sand $2 > \Phi >$ 0.02 mm (%)	Silt $0.02 > \Phi >$ 0.002 mm (%)	Clay $\Phi <$ 0.002 mm (%)
Nsimalen laterite	Yellow, sandy	13.6	43.98	14.51	27.91
Messamendongo laterite	Red, sandy-clayey	10.75	30.53	18.27	40.45
Mbankomo laterite	Red, clayey-sandy	6.33	47.14	11.63	34.89

In the absence of characterization by the Proctor test, the mixing water content was determined using an iterative experimental optimization method. This protocol aimed to identify the optimal plastic consistency required for static compaction and immediate demolding of the compressed earth blocks (CEB). This em-

pirical approach made it possible to reconcile the intergranular lubrication needed for mix workability with the absence of adhesion of the clay matrix to the walls of the metal mold. The optimal water content by mass was 15%. This result falls within the optimum moisture content (OMC) ranges reported for similar clay matrices. The scientific literature indeed reports values between 10% and 15% for non-stabilized composites [30] [31], and up to 18% for cement-stabilized composites [32]. This increase in water content is due to the exothermic hydration reactions of the hydraulic binder. A total of 12 liters of water was used.

The binder used for stabilization is a CP-J 35 composite Portland cement from Cimencam, the characteristics of which are given in **Table 5** below:

Table 5. Characteristics of CP-J 35 Portland cement.

Characteristic	Specification/Value
Commercial designation	CPJ 35/Classique (legacy range) or Multix (depending on product range evolution)
Cement type	Composite Portland cement
Strength class	35 MPa at 28 days (generally standardized ≥ 32.5 MPa)
Main composition	Clinker (≥65%) + secondary additions (limestone, pozzolan) + gypsum (set regulator)
Standard packaging	50 kg bags
Initial setting time	≥90 minutes
Color	Grey

2.2. Properties of Rhecktophyllum Camerunense (RC) Fiber

The characteristics of RC fiber, drawn from the physical and mechanical characterization work of Ntenga (2007) [14] and Betene Ebanda (2012) [15], are as follows:

- Bulk density: ρ_a = 947 kg/m^3
- Average diameter: d = 0.350 mm
- Circularity index: 60.8% - 94.5%
- Longitudinal modulus of elasticity: E = 1.447 to 17.056 GPa
- Tensile strength at failure: R_p = 0.150 to 1.738 GPa

2.3. Formulation and Specimen Preparation

Fibers are introduced into the matrix as a percentage of the dry mass of the control specimen. Four fiber reinforcement rates were defined:

- CEB 0: control matrix without fiber (0%)
- CEB 1: specimen containing 0.5% RC fiber
- CEB 2: specimen containing 1.0% RC fiber
- CEB 3: specimen containing 1.5% RC fiber

For each fiber formulation, three cement stabilization rates were tested: 4%, 6% and 8% relative to the dry soil mass. The reinforcement rate was limited to 1.5% owing to clogging and fiber agglomeration phenomena observed beyond this

value, which prevented homogeneous distribution within the mix.

To prepare our samples, we first had to extract the RC fibers according to a well-defined protocol. The different steps of extracting the fibers from the roots are those used by Ntenga in 2007 [14]. This method is summed up in the following three (3) points:

1) Lightly hand-thresh the RC root;

2) Immerse the threshed roots in a large container of cold water and cover for two weeks (retting). This promotes the rotting of threshed roots;

3) Wait two to three weeks after immersion, then wash the aerial roots thus obtained. This washing removes all the dead skin and reveals the fibers, the fibers obtained are finally dried.

The RC fibers were cut to a length 100 mm and they do not undergo any treatments.

The samples were prepared at room temperature (29˚C). To create them, dry soil was required, which necessitated a preliminary drying process. The soil was dried in an oven for 24 hours at 65˚C. Subsequently, the materials (soil and cement) were first dry-mixed, then blended with water at a moisture content of 15% using a 5-liter cement mixer operating at a speed of 139 rpm. The dry components were homogenized for three minutes, followed by a two-minute mixing period after the addition of water. The mixing water content was 15% by dry mass (Section 2.1). Next, the fibers were added (in a random manner) and mixed in manually for five minutes.

The mix was statically compacted in a metal mold at a pressure of immediately after mixing, under a pressure of 30 kN for 15 seconds, using a digital press of the brand IGM (Ingénierie General des Mesures), reference number S/N: 08061246. And the specimens were demolded immediately after compaction.

After demolding, the specimens were placed in an enclosure and covered for curing for 7, 14 or 28 days at temperature of 24˚C and were tested at the end of the curing period.

2.4. Mechanical and Physical Testing Protocols

Three-point bending test: carried out in accordance with standard NF EN 196-1 [33] on prismatic specimens measuring 160 × 40 × 40 mm^3. The span between the lower supports is set at 100 mm. A constant loading rate of 5 kN/min is applied. Flexural strength is calculated using the formula below, where F is the breaking force, l the width of the specimen, e the thickness of the specimen, and d the distance between the two points:

$$R_f = \frac{3 \times F \times l}{2 \times b \times d^2} \quad (1)$$

Uniaxial compression test: performed on 40 × 40 × 40 mm cubic specimens obtained from the flexural-test fragments (in accordance with standard NF EN 196-1). A hydraulic press applies a monotonic load at a rate of 5 kN/min until failure. Strength is calculated using the formula below, where F is the compressive

force and A the area of the compressed section:

$$R_c = \frac{F}{A} \tag{2}$$

Physical tests (bulk density, absorption and porosity): the dry-state bulk density is measured geometrically by weighing and dimensional measurement with calipers. The formula is as follows:

$$\rho = \frac{M}{V} \tag{3}$$

The water absorption rate (Abs%) is determined after oven-drying at 103˚C for 24 h (to obtain the dry mass M_s), followed by complete immersion in water for 24 h (saturated mass M_t), using the following equation in accordance with standard ASTM C373 [34]:

$$\text{Abs}\% = \left[\frac{M_t - M_s}{M_s}\right] \times 100 \tag{4}$$

Apparent porosity (P%) is derived from the same measurements. The reference method in ASTM C373 defines apparent porosity from the dry, saturated and water-suspended (Archimedes) masses; as no suspended-mass (hydrostatic) weighing was performed in this study, porosity is instead estimated from the water absorption and the dry bulk density, following common practice when the Archimedes measurement is unavailable:

$$\text{P}\% = \text{Abs}\% \times \rho \tag{5}$$

where ρ is the dry bulk density in g/cm^3 (Equation (3)). Tests were conducted at curing ages of 7, 14 and 28 days.

2.5. Statistical Treatment

As highlighted in Section 1, systematic reviews of the CEB literature note that studies on fiber- and stabilizer-reinforced blocks generally omit formal statistical treatment of replicate measurements [17]. To address this gap, the mechanical and physical results (density, water absorption, porosity, R_c, R_f) for each formulation, including the unreinforced control (CEB 0, 0% fiber), are reported as the mean ± standard deviation of n = 5 replicate specimens per laterite × fiber content × cement dosage × curing-age cell (Section 3, **Figures 5-9**). CEB 0 was tested under the same conditions as the reinforced formulations, with five replicate prisms per cell (raw data in the companion spreadsheet). The inferential analysis consists of a two-way analysis of variance (ANOVA) performed separately for each property and for each laterite × curing-age series (3 laterites × 3 curing ages = 9 series), with fiber content (four levels: 0%, 0.5%, 1% and 1.5%, the 0% level being CEB 0) and cement dosage (three levels: 4%, 6% and 8%) as fixed factors, including their interaction (12 cells of n = 5 per series). Each series was analyzed independently; no analysis was grouped by laterite × cement dosage, and every fiber-content or cement-dosage effect reported in Section 3 comes from this analysis. The normal-

ity of model residuals was assessed by the Shapiro-Wilk test and variance homogeneity by Levene's test. Dunnett's test was used to compare each reinforced formulation (0.5%, 1% and 1.5% fiber) with the matched CEB 0 (same laterite, cement dosage and curing age; 3 comparisons × 27 matched sets = 81 comparisons per property), and Tukey's honestly significant difference (HSD) post-hoc test to identify which pairs of fiber contents or cement dosages differ significantly among the reinforced formulations, at a significance threshold of $\alpha = 0.05$.

The mechanical properties of the reinforced compressed earth blocks (CEBs) were determined in accordance with the operating procedures of standard EN 196-1, adapted to prismatic specimens measuring 4 × 4 × 16 cm. For each combination of "laterite type × curing age × cement content", n = 5 independent prisms (experimental units) were tested. Although cast consecutively from a single homogeneous mix per formulation, each prism was handled independently during the curing and failure stages in order to ensure the statistical independence of the measurements.

Each experimental unit (4 × 4 × 16 cm) was first subjected to the three-point flexural strength test (R_f). Since flexural failure produced two fragments per prism, these two half-prisms were immediately tested in simple compression (R_c) using a standard compression device fitted to the 4 × 4 cm faces. To avoid any pseudo-replication in the analysis of variance (ANOVA), the arithmetic mean of the compressive strengths of the two fragments from the same prism was calculated. This mean value represents the single measurement of R_c assigned to that experimental unit, thereby preserving the balanced design with true replicates used for the formal statistical treatments.

Across the five properties and nine laterite × curing-age series analyzed, model residuals passed the Shapiro-Wilk normality test in 33% of series and variance homogeneity (Levene) was satisfied in 89% of series; ANOVA and Tukey results are reported nonetheless, following common practice for moderately sized, balanced designs (n = 5 per cell), and should be read as approximate rather than exact for the series in which normality is rejected. With CEB 0 included, the fiber-content effect was statistically significant ($p < 0.05$) for all five properties in all nine series ($p < 0.001$ for R_c and R_f in every series). Dunnett's test against the matched CEB 0 is significant for all 81 reinforced comparisons for R_c (gains of +81% to +271%, median +151%) and for R_f (gains of +398% to +684%, median +577%), with $p < 0.001$ throughout. For the physical properties, the response to fibers is mixed: 30 of the 81 comparisons are significant for bulk density (all decreases; changes ranging from −12% to +1%), 31 for water absorption (25 increases, 6 decreases) and 26 for porosity (p = Abs% × dry density, Equation (5); 17 increases, 9 decreases). Full ANOVA tables, Shapiro-Wilk/Levene diagnostics and pairwise Dunnett and Tukey comparisons for every property × laterite × curing-age combination are provided in the companion spreadsheet. The strength improvements over CEB 0 reported in this paper are therefore statistically established for R_c and R_f, whereas differences in the physical properties should be read cell by cell.

3. Results and Discussion

3.1. Evolution of Bulk Density

The experimental values of dry-state bulk density (in kg/m³) for the different formulations are presented in Figure 5.

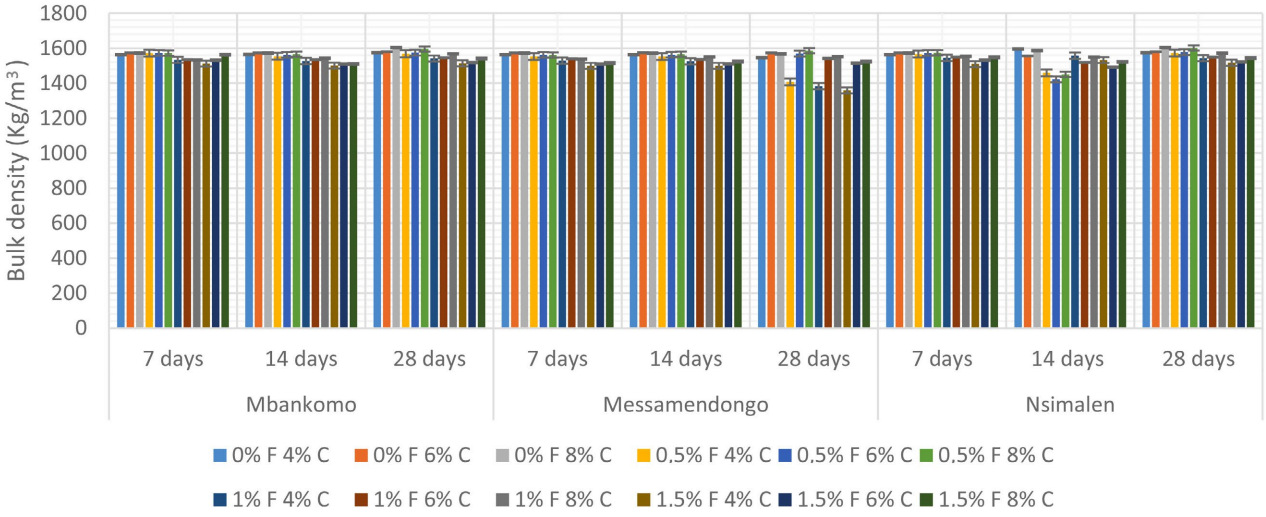


Figure 5. Bar chart of bulk density variation (error bars: ± SD, n = 5, where available).

At 0% fiber (CEB 0), the Mbankomo laterite gives the maximum bulk density at 8% cement after 28 days of curing (1603.2 kg/m³). Among the reinforced composites, the best compactness is obtained with the Nsimalen laterite at 8% cement and 0.5% fiber (1600.9 ± 22.5 kg/m³), closely followed by the Mbankomo laterite under the same conditions (1595.8 ± 24.2 kg/m³) - both essentially matching the unreinforced control. As fiber content increases beyond 0.5%, bulk density decreases monotonically for all three laterites, consistent with the low intrinsic density of the plant fibers relative to the mineral grains and with the creation of microcavities at the fiber/matrix interface.

3.2. Kinetics of the Water Absorption Rate

The water absorption test results are compiled in Figure 6.

Without fibers, the highest absorption rate (21.033%) is observed at 4% cement with the Nsimalen laterite at 7 days of curing. Among the reinforced specimens (0.5%, 1% and 1.5% fiber, for which replicate data are available), absorption increases monotonically with fiber content at every cement dosage and every laterite - for example, from 18.2% to 21.2% at 7 days for Nsimalen at 4% cement as fiber content rises from 0.5% to 1.5%. This behavior is correlated with the intrinsically hydrophilic nature of the plant cellulose fibers and is confirmed by a statistically significant fiber effect (two-way ANOVA among the reinforced formulations, fiber content × cement dosage: fiber effect $p < 0.05$ in 8 of 9 laterite × curing-age series; see Section 2.5). With curing time (14 and 28 days), absorption decreases

as the cement hydration reactions progress and clog the pores.

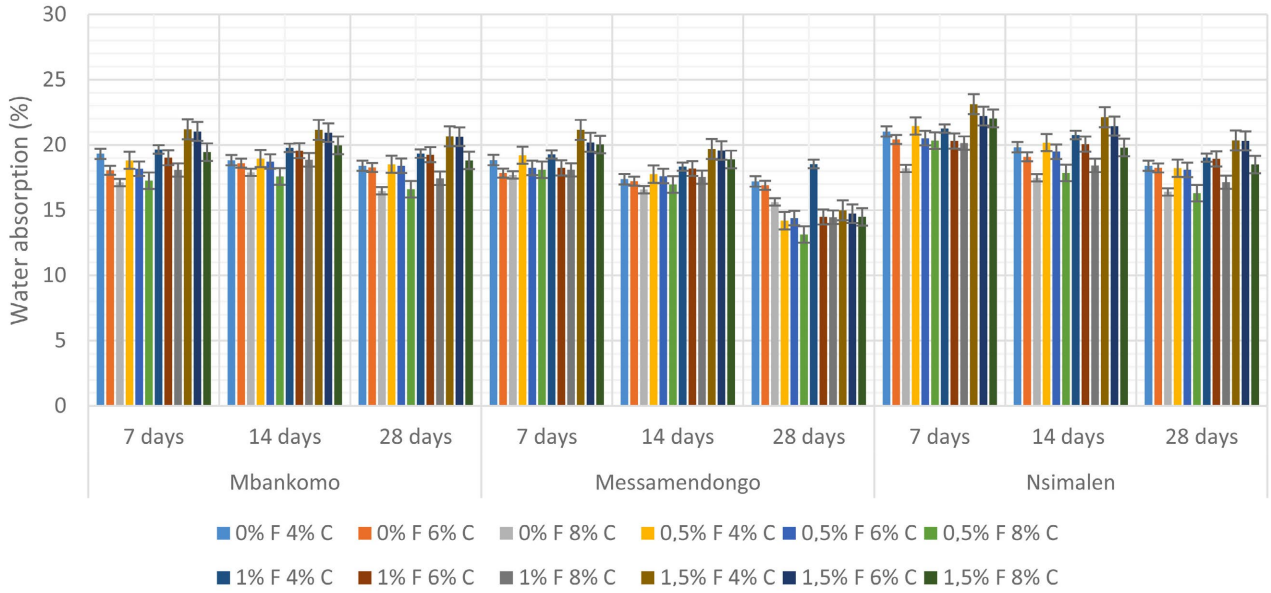


Figure 6. Bar chart of the water absorption rate (error bars: ± SD, n = 5, where available).

3.3. Porosity Analysis

The porosity calculation results are given in Figure 7. As detailed in Section 2.4, porosity is computed as p (%) = Absorption (%) × dry bulk density (g/cm^3)—the standard approximation when no hydrostatic (Archimedes) weighing is available.

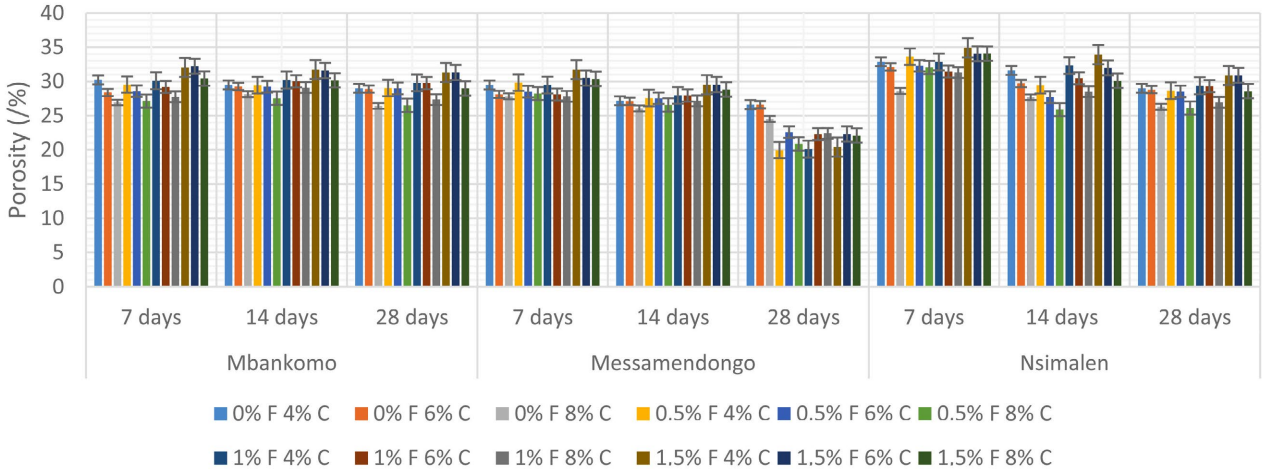


Figure 7. Bar chart of porosity, p = Absorption × dry density (error bars: ± SD, n = 5, where available).

With the corrected formula, porosity values are markedly higher than in the raw file's own (dimensionally inconsistent) computation—in the 25% - 35% range rather than 9% - 15%—but the qualitative trends are unchanged or, in places, clarified. For the unreinforced matrix (CEB 0), the highest porosity is now found for the Nsimalen laterite at 4% cement at 7 days of curing (32.9%), followed closely

by Nsimalen at 6% cement (32.1%); the Messamendongo 4%/7-day cell that appeared highest under the raw file's formula (29.4%) is not the maximum once the formula is corrected. Among the reinforced specimens, porosity at Mbankomo /4% cement rises only mildly from 0.5% to 1% fiber (29.0% → 29.8% at 28 days, against 29.0% for CEB 0) but increases more clearly at 1.5% fiber (31.3%), consistent with the clogging-effect hypothesis. The single highest value among all reinforced specimens is the Nsimalen laterite at 4% cement and 1.5% fiber at 7 days (34.9% ± 1.1%). Averaged across all laterites and cement dosages at 28 days, mean porosity rises modestly and monotonically with fiber content (25.7% at 0.5%, 26.4% at 1%, 27.4% at 1.5%, against 27.3% for CEB 0), supporting the interpretation that macroscopic interstitial voids accumulate progressively with fiber loading, most visibly beyond about 1%.

3.4. Uniaxial Compressive Strength (R_c)

The compression test results are given in Figure 8.

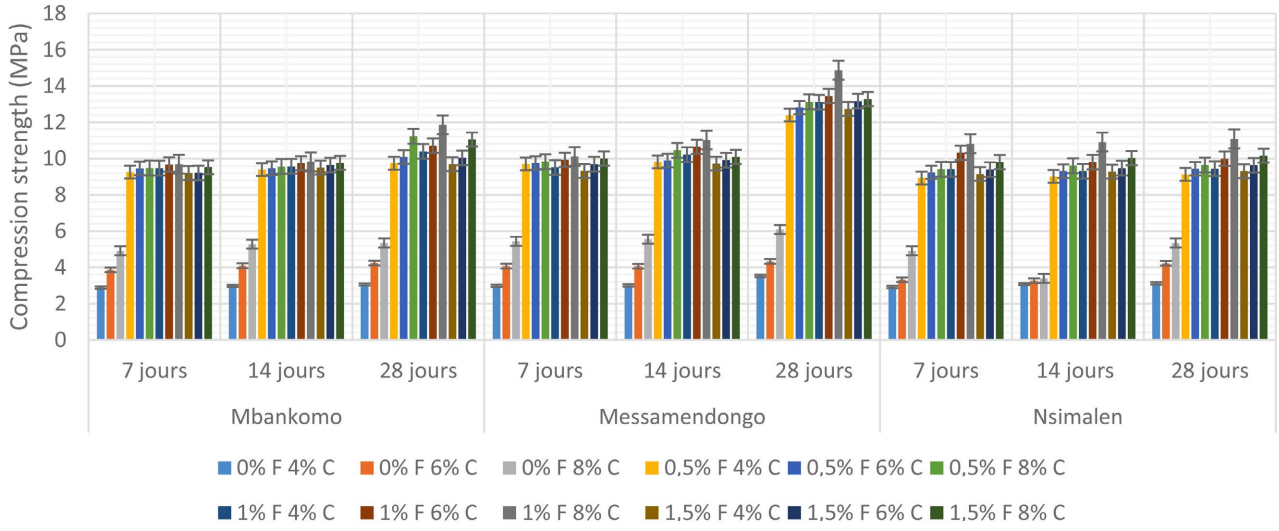


Figure 8. Bar chart of compressive strength (error bars: ± SD, n = 5, where available).

Compressive strength increases markedly with cement content, and the reinforced formulations (CEB 1 - CEB 3) show markedly higher values than the unreinforced control CEB 0; Dunnett's test against the matched CEB 0 shows that this difference is statistically significant ($p < 0.001$) in all 81 comparisons (gains of +81% to +271%). For all formulations, the absolute maximum value is measured with the Messamendongo laterite at 28 days of curing, with 8% cement and 1% RC fiber (CEB 2): 14.87 ± 0.12 MPa (n = 5). A two-way ANOVA including CEB 0 (fiber content 0% - 1.5% × cement dosage, Section 2.5) shows that both factors have a statistically significant effect on R_c in every laterite × curing-age series ($p < 0.001$ in all 9 series). Increasing fiber content from 1% to 1.5% lowers R_c in 26 of 27 laterite × cement × age combinations; Tukey's HSD test among the reinforced formulations finds this decrease statistically significant at 28 days for the Mes-

samendongo (−0.75 MPa, p = 0.0015) and Mbankomo (−0.73 MPa, p = 0.017) laterites, but not for Nsimalen (p = 0.059), indicating a real but laterite-dependent saturation effect rather than a uniformly significant one. This phenomenon is attributed to the predominance of the elasticity effect induced by excess fiber and to the weakness of the interfacial transition zones created by the voids, which reduces the effectiveness of the hydrated cementitious matrix.

In absolute terms, this 14.87 MPa peak places RC fiber-reinforced CEB at the upper end of the range reported for natural fiber-reinforced compressed earth blocks (Table 1); the compressive strengths typically reported for sisal-cement CEB cluster between about 4 and 13.44 MPa depending on soil type and fiber treatment [22] [23]. Absolute strengths are, however, not a valid basis for ranking fibers, because they depend on soil, cement dosage, curing time and specimen geometry. Gains must instead be expressed as percentages relative to unreinforced controls matched in laterite, cement dosage and curing time. For the optimal RC formulation, the matched control (CEB 0, Messamendongo laterite, 8% cement, 28 days) gave 6.09 ± 0.18 MPa (n = 5), which corresponds to a gain of (14.87 − 6.09)/6.09 = +144.1% (Dunnett, p < 0.001). For the same laterite and curing age with 1% fiber, the gains over the matched controls are +271.3% at 4% cement (13.11 vs. 3.53 MPa), +211.0% at 6% cement (13.45 vs. 4.33 MPa) and +144.1% at 8% cement, all significant at p < 0.001. The gain thus decreases as the cement dosage, and hence the strength of the control, increases. The +43.6% gain reported for bamboo fiber [17] was obtained against its own unreinforced matrix, with a different soil and stabilization, so it can be compared with these figures only qualitatively, and no superiority of RC fiber over bamboo is claimed. The 1% optimal fiber content identified here is also consistent with the 0.4 wt% - 1.0 wt% optimum window reported across the sisal, kenaf and bamboo literature [17] [22] [23].

3.5. Three-Point Flexural Strength (R_f)

The flexural strength values are grouped in Figure 9.

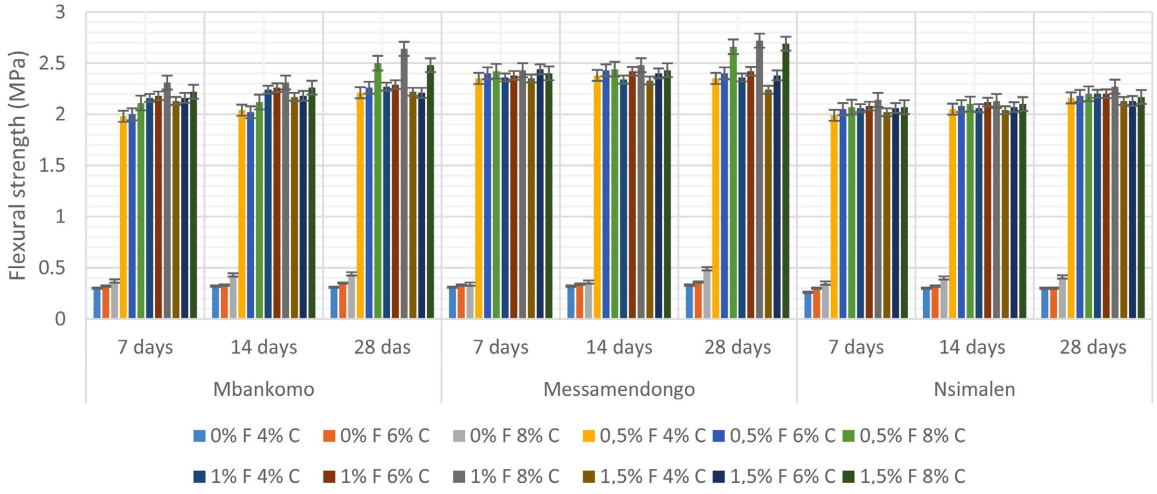


Figure 9. Bar chart of flexural strength (error bars: ± SD, n = 5, where available).

Flexural strength is substantially higher in the reinforced formulations than in the unreinforced control: the matched CEB 0 control (Messamendongo, 8% cement, 28 days) gave 0.49 ± 0.04 MPa (n = 5), against 2.72 ± 0.09 MPa (n = 5) for the optimal formulation (same laterite, cement dosage and age, 1% fiber), a gain of +455% (Dunnett, $p < 0.001$). With CEB 0 included, the fiber-content effect on R_f is statistically significant in all 9 laterite × age ANOVA series ($p < 0.001$); among the reinforced formulations alone it is significant in 6 of the 9 series ($p < 0.05$), including at 28 days for all three laterites; after Tukey correction among the reinforced formulations, however, the 1% - 1.5% decrease at 28 days specifically reaches significance only for the Nsimalen laterite ($p = 0.014$). This performance is explained by the load-transfer and microcrack-bridging mechanism provided by the fiber network, consistent with the crack-bridging role reported for sisal, kenaf and jute fibers in earlier CEB studies [16] [17]. As with compressive strength, the decrease beyond 1% fiber is directionally consistent (26 of 27 combinations) but not uniformly significant across laterites, owing to the formation of local clusters of poorly coated fibers that act as stress concentrators a saturation effect also documented for jute- and kenaf-reinforced CEB beyond their respective optimal contents [16] [17].

4. Conclusions

This experimental study characterized the influence of reinforcement with the tropical plant fiber Rhecktophyllum camerunense (RC), combined with cement stabilization, on the physical and mechanical properties of CEBs produced from three Yaoundé laterites. The main conclusions are as follows:

1) The introduction of RC fibers reduces the overall bulk density owing to the low density of the biomass and the local increase in interstitial porosity.

2) The water absorption kinetics are initially heightened at 7 days by the hydrophilic nature of the cellulose fiber, before decreasing under the effect of continued cement hydration at 28 days.

3) The flexural and compressive strengths of the reinforced formulations are considerably higher than those of the unreinforced control (CEB 0): Dunnett's test against the matched CEB 0 is significant ($p < 0.001$) in all 81 comparisons for both properties, with gains of +81% to +271% in compression and +398% to +684% in flexion. The optimal formulation is identified for the Messamendongo laterite with 8% cement and 1% RC fiber at 28 days of curing, showing peak performances of 14.87 MPa (compression) and 2.72 MPa (flexion).

4) A saturation threshold content of 1% fiber was identified. Beyond this value (1.5%), agglomeration and clogging phenomena impair microstructural homogeneity, resulting in decreased strength; this decrease is directionally consistent across 26 of 27 laterite × cement × age combinations for both R_c and R_f, and reaches statistical significance (Tukey HSD, $p < 0.05$) for at least one laterite at 28 days for each property.

5) Benchmarked against the recent literature on natural fiber-reinforced CEB

(sisal, kenaf, jute, bamboo, Alfa), the RC fiber system studied here ranks among the higher-performing formulations reported to date, while confirming the cross-fiber recurrence of a saturation threshold near 1 wt%.

Further investigations, in particular by Scanning Electron Microscopy (SEM), are needed to study the fiber/matrix interfacial transition zone (ITZ) and to analyze the long-term chemical durability of these plant fibers within the alkaline environment induced by cement. One limitation should be addressed before submission: the apparent-porosity formula used in the source data should be reconciled with the laboratory notebook (Section 2.4).

Author Contributions

Jaques Bertrand SOMBGA: conducted the experiments, processed and analyzed the results, and subsequently drafted the document.

Jean Calvin BIDOUNG and Lucien MEVA'A contributed to the interpretation of the results and the review of the document.

Conflicts of Interest

The authors declare no conflicts of interest regarding the publication of this paper.

References

[1] Fujii, Y., Fodde, E., Watanabe, K. and Murakami, K. (2009) Digital Photogrammetry for the Documentation of Structural Damage in Earthen Archaeological Sites: The Case of Ajina Tepa, Tajikistan. *Engineering Geology*, **105**, 124-133. https://doi.org/10.1016/j.enggeo.2008.11.012

[2] Quagliarini, E. (2006) Earth Construction in the Marche Region (Italy): Building Techniques and Materials. *Proceedings of the Second International Congress on Construction History*, Cambridge, 29 March-2 April 2006, 2559-2572. https://iris.univpm.it/handle/11566/224560

[3] Soles, J.S. and Davaras, C. (1994) Excavations at Mochlos, 1990-1991. *Hesperia*, **63**, 391-436. https://doi.org/10.2307/148208

[4] Quagliarini, E., Lenci, S. and Iorio, M. (2010) Mechanical Properties of Adobe Walls in a Roman Republican Domus at Suasa. *Journal of Cultural Heritage*, **11**, 130-137. https://doi.org/10.1016/j.culher.2009.01.006

[5] Houben, H. and Guillaud, H. (1989) Earth Construction: Comprehensive Treatise. CRATerre, Éditions Parenthèses. https://editionsparentheses.com

[6] Houben, H. and Guillaud, H. (2006) Traité de Construction en Terre. CRATerre, Éditions Parenthèses https://editionsparentheses.com

[7] Saadi, I. and Belouettar, R. (2011) Mechanical Behavior of Raw Earth Bricks Reinforced with Date Palm Fibers and Straw Fibers. INVACO2 International Seminar, Innovation & Valorization in Civil Engineering & Building Materials, 2p-118.

[8] Taallah, B. (2014) Study of the Physico-Mechanical Behavior of Compressed Earth Blocks with Fibers. Ph.D. Thesis, University Mohamed Khider. https://univ-biskra.dz

[9] Mostafa, M. and Uddin, N. (2016) Experimental Analysis of Compressed Earth Block (CEB) with Banana Fibers Resisting Flexural and Compression Forces. *Case Studies in Construction Materials*, **5**, 53-63. https://doi.org/10.1016/j.cscm.2016.07.001

[10] Ismail, S. and Yaacob, Z. (2011) Properties of Laterite Brick Reinforced with Oil Palm Empty Fruit Bunch Fibres. *Pertanika Journal of Science & Technology*, **19**, 31-41. https://semanticscholar.org

[11] Taallah, B., Guettala, A., Guettala, S. and Kriker, A. (2014) Mechanical Properties and Hygroscopicity Behavior of Compressed Earth Block Filled by Date Palm Fibers. *Construction and Building Materials*, **59**, 161-168. https://doi.org/10.1016/j.conbuildmat.2014.02.058

[12] Saleem, M.A., Abbas, S. and Haider, M. (2016) Jute Fiber Reinforced Compressed Earth Bricks (FR-CEB)—A Sustainable Solution. *Pakistan Journal of Engineering and Applied Sciences*, **19**, 83-90. https://doi.org/10.67635/pjeas.2016.19.1.302

[13] Ntépé, C. (1980) Une Nouvelle Espèce Pour Le Genre Rhektophyllum N. E. Brown (Araceæ). *Adansonia*, **20**, 451-457. https://doi.org/10.5962/p.297220

[14] Ntenga, R. (2007) Multi-Scale Modeling and Characterization of the Elastic Anisotropy of Tropical Plant Fibers for Composite Material Reinforcement. Ph.D .Thesis, Université Blaise Pascal. https://hal.science

[15] Betene Ebanda, F. (2012) Étude des propriétés mécaniques et thermiques du plâtre renforcé de fibres végétales tropicales. Ph.D. Thesis, Université Blaise Pascal. https://hal.science

[16] Laborel-Préneron, A., Aubert, J.E., Magniont, C., Tribout, C. and Bertron, A. (2016) Plant Aggregates and Fibers in Earth Construction Materials: A Review. *Construction and Building Materials*, **111**, 719-734. https://doi.org/10.1016/j.conbuildmat.2016.02.119

[17] Valenzuela, M., Ciudad, G., Cárdenas, J.P., Medina, C., Salas, A., Oñate, A., et al. (2024) Towards the Development of Performance-Efficient Compressed Earth Blocks from Industrial and Agro-Industrial By-Products. *Renewable and Sustainable Energy Reviews*, **194**, Article ID: 114323. https://doi.org/10.1016/j.rser.2024.114323

[18] Jesudass, A., Gayathri, V., Geethan, R., Gobirajan, M. and Venkatesh, M. (2021) Earthen Blocks with Natural Fibres—A Review. *Materials Today*: *Proceedings*, **45**, 6979-6986. https://doi.org/10.1016/j.matpr.2021.01.434

[19] Subramanian, G.K.M., Balasubramanian, M. and Jeya Kumar, A.A. (2021) A Review on the Mechanical Properties of Natural Fiber Reinforced Compressed Earth Blocks. *Journal of Natural Fibers*, **19**, 7687-7701. https://doi.org/10.1080/15440478.2021.1958405

[20] Mora-Ruiz, V., Soto-Paz, J., Attia, S. and Mejía-Parada, C. (2025) Sustainable Earthen Construction: A Meta-Analytical Review of Environmental, Mechanical, and Thermal Performance. *Buildings*, **15**, Article 918. https://doi.org/10.3390/buildings15060918

[21] Bailly, G.C., El Mendili, Y., Konin, A. and Khoury, E. (2024) Advancing Earth-Based Construction: A Comprehensive Review of Stabilization and Reinforcement Techniques for Adobe and Compressed Earth Blocks. *Eng*, **5**, 750-783. https://doi.org/10.3390/eng5020041

[22] Labiad, Y., Meddah, A. and Beddar, M. (2022) Physical and Mechanical Behavior of Cement-Stabilized Compressed Earth Blocks Reinforced by Sisal Fibers. *Materials Today: Proceedings*, **53**, 139-143. https://doi.org/10.1016/j.matpr.2021.12.446

[23] Abinaya, A., Kumar, S., Muthu, M. and Thomas, B.S. (2023) Compressed Earth Block Reinforced with Sisal Fiber and Stabilized with Cement: Manual Compaction Procedure and Influence of Addition on Mechanical Properties. *Materials Today*: *Proceedings*.

[24] Labiad, Y., Meddah, A. and Beddar, M. (2023) Performance of Sisal Fiber-Reinforced

Cement-Stabilized Compressed-Earth Blocks Incorporating Recycled Brick Waste. *Innovative Infrastructure Solutions*, **8**, Article No. 107. https://doi.org/10.1007/s41062-023-01078-w

[25] Gorisse, F. (1978) Essais et contrôle des bétons, Vol. 2. Eyrolles.

[26] Rigassi, V. (1995) Compressed Earth Blocks: Volume I: Manual of Production. CRA-Terre-EAG, GATE, 1-104. https://craterre.hypotheses.org/290

[27] Izemmouren, W., Guettala, A. and Gadri, K. (2013) Effect of Curing Conditions on the Physical and Mechanical Properties of Compressed Earth Blocks. *Actes du XXIe Congrès Français de Mécanique*, Bordeaux, 26-30 August 2013, 1-6. https://hal.science

[28] AFNOR (2022) Compressed Earth Blocks for Walls and Partitions-Definitions-Specifications-Test Methods-Delivery Acceptance Conditions (XP P13-901). AFNOR. https://afnor.org

[29] Association Française de Normalisation (AFNOR) (2018) Sols: Reconnaissance et Essais-Détermination des Limites d'Atterberg. Limite de Liquidité à la Coupelle. Limite de Plasticité au Rouleau; Standard No. NF P 94-051. AFNOR. https://afnor.org

[30] Houben, H. and Guillaud, H. (1994) Earth Construction: A Comprehensive Guide. Intermediate Technology Publications, 1-362.

[31] Bahar, R., Benazzoug, M. and Kenai, S. (2004) Performance of Compacted Cement-Stabilised Soil. *Cement and Concrete Composites*, **26**, 811-820. https://doi.org/10.1016/j.cemconcomp.2004.01.003

[32] Walker, P.J. (1995) Strength, Durability and Shrinkage Characteristics of Cement Stabilised Soil Blocks. *Cement and Concrete Composites*, **17**, 301-310. https://doi.org/10.1016/0958-9465(95)00019-9

[33] Association Française de Normalisation (AFNOR) (2016) Methods of Testing Cement-Part 1: Determination of Strength; Standard No. NF EN 196-1. AFNOR. https://www.boutique.afnor.org/en-gb/standard/nf-en-1961/methods-of-testing-cement-part-1-determination-of-strength/fa184622/57803

[34] ASTM International (2006) Standard Test Method for Water Absorption, Bulk Density, Apparent Porosity, and Apparent Specific Gravity of Fired Whiteware Products (ASTM C373-88, Reapproved 2006). ASTM International.